A note on the MUSIC algorithm for impedance tomography

Martin Hanke

Institut für Mathematik, Johannes Gutenberg-Universität, 55099 Mainz, Germany

E-mail: hanke@math.uni-mainz.de

Abstract. We investigate the MUSIC algorithm for the reconstruction of small (infinitesimal) inclusions inside a planar homogeneous object from discrete impedance tomography data within the framework of the gap electrode model. We provide a justification of the method whenever the number of electrodes exceeds $2(J+1)$ where J is the number of the inclusions to be found.

AMS classification scheme numbers: 65N21, 35R30

1. Introduction

MUSIC, an acronym for **mu**ltiple **si**gnal **c**lassification, is an established technique in signal processing, cf., e.g., Therrien [12]. In the inverse scattering community Devaney [5] (see also [6]) adapted this technique in the late 1990's to the reconstruction of point scatterers, and in the summer of 2000, while my former student Martin Brühl was visiting Michael Vogelius at Rutgers, the two of them observed that similar ideas also work well to localize small (infinitesimal) inclusions inside a homogeneous object from electrical impedance tomography data. Based on the results in [4] Michael provided the theoretical backbone for this method, namely that the associated Neumann-Dirichlet map is, essentially, a finite rank perturbation of the reference Neumann-Dirichlet operator; this rank amounts to dJ, i.e., the space dimension $d \geq 2$ times the number J of the small inclusions. Eventually, this collaboration led to our joint paper [3]; my own contribution was comparatively minor and consisted in the exclusion of false-negative reconstructions.

Later, we extended the method to also treat limited angle data and finite electrode configurations [8], and together with Habib Ammari and Roland Griesmaier we drew connections to the so-called factorization method [1, 7].

Apparently unaware of [8], Lechleiter [10] very recently reconsidered this MUSIC variant of electrical impedance tomography for finite electrode configurations. The novel result in [10] is a justification of the algorithm for this discrete situation in two and three space dimensions when the number of (point) electrodes goes to infinity and their boundary positions become everywhere dense; see [10] for the precise statement. A shortcoming of the technique used in [10] is that the number N of electrodes that are required to reconstruct a given configuration of finitely many inclusions is not known before-hand.

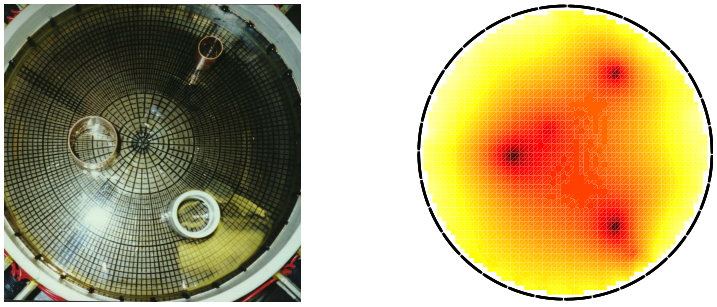

Figure 1. Phantom (left) and MUSIC reconstruction (right). Figure reprinted from [8].

The purpose of this note is to show that in two space dimensions a significantly stronger result is valid, namely, that when there are J (infinitesimal) inclusions in the object then all of them, and no false-positives, will be reconstructed with $N = 2J + 3$ (or more) electrodes, wherever they are attached to the boundary. Moreover, we show that if only $N = 2J + 2$ (or less) electrodes are being used then false-positive reconstructions are possible; when $N \leq 2J$ then false-negatives can also occur. These results not only apply to point electrodes but also to the more general gap model for finite (i.e., positive) size electrodes.

We like to emphasize that our results (like those in [10]) ignore the influence of noise and are formulated for an asymptotic model of infinitesimal inclusions to be specified in Section 2. Also, at the time of writing we don't know whether the same or similar results can also be established for even more realistic electrode models described, e.g., in Mueller and Siltanen [11], like the shunt or the complete electrode model. Numerical experiments with real data, however, are very encouraging. To support this latter statement we reproduce here a numerical example from [8] for real data. Figure 1 shows the tank of a measurement device from Rensselaer Polytechnic Institute, Troy, NY, with $N = 32$ electrodes and a phantom consisting of $J = 3$ inclusions, namely a piece of plastic and two metal objects. Note that these objects are not 'infinitesimal'. The right-hand side plot is the corresponding output of the MUSIC algorithm; see [8] for a more detailed description of this example.

2. Setting of the problem

The mathematical formulation of the impedance tomography problem is based on the boundary value problem

$$-\nabla \cdot (\sigma \nabla u) = 0 \quad \text{in } D\,, \qquad \partial_\nu u = f \quad \text{on } \partial D\,, \tag{2.1}$$

cf., e.g., [11], where D is a bounded and simply connected Lipschitz domain in $\mathbb{R}^2$, and ∂_ν denotes the outer normal derivative on its boundary ∂D. We assume that the conductivity σ is equal to one except for some subdomains $\Omega_j \subset D$, $j = 1, \ldots, J$, where the conductivity attains constant positive values $\sigma_j \neq 1$, i.e.,

$$\sigma = \begin{cases} \sigma_j & \text{in } \Omega_j\,,\ j = 1, \ldots, J\,, \\ 1 & \text{else}\,. \end{cases}$$

These subdomains are presumed to be small; to be specific we consider the case that

$$\Omega_j \,=\, x_j \,+\, \varepsilon\mathcal{O}_j\,, \qquad j=1,\ldots,J\,, \tag{2.2}$$

where $x_j \in D$ are the pairwise different centers of mass of Ω_j, $\mathcal{O}_j$ are C^2 smooth bounded and simply connected domains, and the scaling parameter $\varepsilon > 0$ is sufficiently close to zero. We refer to x_j as the position of the obstacle Ω_j and to $\mathcal{O}_j$ as its shape.

Denote by $L^2_\diamond(\partial D)$ the set of L^2 functions over ∂D with vanishing mean and by $H^1_\diamond(D)$ the set of H^1 functions over D with trace in $L^2_\diamond(\partial D)$. Then it is well known that for $f \in L^2_\diamond(\partial D)$ the boundary value problem (2.1) has a unique weak solution $u \in H^1_\diamond(D)$. The selfadjoint operator

$$\Lambda_\varepsilon : L^2_\diamond(\partial D) \to L^2_\diamond(\partial D)\,, \qquad \Lambda_\varepsilon : f \mapsto g = u|_{\partial D}\,,$$

which takes the boundary current f onto the trace of the solution u of (2.1) is known as the Neumann-Dirichlet operator associated with this conductivity σ; we also introduce the corresponding Neumann-Dirichlet operator Λ_0 for the homogeneous conductivity $\sigma_0 \equiv 1$. The main result of [3] states that

$$\Lambda_\varepsilon - \Lambda_0 \,=\, \varepsilon^2 K + o(\varepsilon^2)\,, \qquad \varepsilon \to 0\,, \tag{2.3}$$

where K is a selfadjoint operator of rank $2J$, which does not depend on ε. Moreover, if $N(x,y)$ is the Neumann function for the Laplacian in D and

$$u_{z,p} \,=\, p \cdot \nabla_y N(\,\cdot\,, z) \tag{2.4}$$

is the corresponding insulated dipole potential sitting in $z \in D$ with dipole moment $p \in \mathbb{R}^2$ and trace

$$h_{z,p} \,=\, u_{z,p}\big|_{\partial D}$$

then

$$h_{z,p} \in \mathcal{R}(K)\,, \qquad \text{if and only if} \qquad z \in \{x_j\}\,. \tag{2.5}$$

In fact, cf. [3], these dipole potentials span the entire range of K, i.e.,

$$\mathcal{R}(K) \,=\, \text{span}\{h_{x_j,p} \,:\, j=1,\ldots,J\,,\ p \in \mathbb{R}^2\}\,. \tag{2.6}$$

These results extend to the case when some inclusions are insulating and others are perfectly conducting; see Ammari and Kang [2].

In the sequel we assume that N electrodes are attached to the boundary of the object D, each of which covering a (relatively closed) connected piece $E_n \subset \partial D$, $n=1,\ldots,N$, with $E_n \cap E_m = \emptyset$ for $n \neq m$; by $|E_n|$ we denote the arc length of E_n. Let $\mathbb{R}^N_\diamond$ be the vectors of $\mathbb{R}^N$ whose entries sum up to zero, and let P be the operator

$$P : L^2_\diamond(\partial D) \to \mathbb{R}^N_\diamond\,, \qquad P : g \mapsto [G_n]_n\,, \tag{2.7}$$

where

$$G_n \,=\, \frac{1}{|E_n|}\int_{E_n} g\,\mathrm{d}s \,-\, c_g \tag{2.8}$$

and

$$c_g \,=\, \frac{1}{N}\sum_{n=1}^{N}\frac{1}{|E_n|}\int_{E_n} g\,\mathrm{d}s\,.$$

The adjoint $P^* : \mathbb{R}^N_\diamond \to L^2_\diamond(\partial D)$ of P maps the vector $I = [I_n]_n \in \mathbb{R}^N_\diamond$ onto the function

$$f \,=\, P^*I \,=\, \begin{cases} I_n/|E_n| & \text{on } E_n\,,\ n=1,\ldots,N\,,\\ 0 & \text{else}\,. \end{cases} \tag{2.9}$$

Assume now that $I = [I_n]_n \in \mathbb{R}^N_\diamond$ and that I_n units of current are simultaneously injected through the electrodes E_n, $n = 1, \ldots, N$, respectively. Defining $G = [G_n]_n = Pg$, where g is the trace of the solution u of (2.1) for the boundary current f of (2.9), then, according to the gap electrode model (cf. [11]), G provides the corresponding potential measurements at the N electrodes, i.e., $G_n - G_m$ is the voltage difference between the nth and the mth electrode.

Accordingly, in the gap model framework $P\Lambda_\varepsilon P^*$ is the discrete measurement operator analog of the continuous Neumann-Dirichlet map considered before, and

$$P\Lambda_\varepsilon P^* - P\Lambda_0 P^* \,=\, \varepsilon^2 PKP^* + o(\varepsilon^2)\,, \qquad \varepsilon \to 0\,,$$

is the gap model analog of (2.3). The corresponding (idealized) MUSIC method consists in testing whether $Ph_{z,p} \in \mathcal{R}(PKP^*)$ for a test point $z \in D$ and some dipole moment $p \in \mathbb{R}^2 \setminus \{0\}$; compare (2.5).† The following general result determines necessary assumptions for the success of this scheme.

Proposition. *Let $D \subset \mathbb{R}^2$ be a bounded and simply connected domain; let K be defined as above and P be any bounded operator from $L^2_\diamond(\partial D)$ to some Hilbert space $\mathcal{X}$. Then the following holds:*

(i) If P is injective on the $2J$ dimensional space (2.6) *then $Ph_{x_j,p} \in \mathcal{R}(PKP^*)$ for every $j = 1, \ldots, J$ and $p \in \mathbb{R}^2$.*

(ii) If P is injective on the set of linear combinations of any $J+1$ insulated dipoles located in D then

$$Ph_{z,p} \in \mathcal{R}(PKP^*)\,, \qquad \text{if and only if} \qquad z \in \{x_j\}\,.$$

Proof. We trivially conclude from (2.6) that

$$\mathcal{R}(PKP^*) \,\subset\, \mathcal{R}(PK) \,=\, \text{span}\{Ph_{x_j,p} \,:\, j = 1, \ldots, J\,,\; p \in \mathbb{R}^2\}\,. \tag{2.10}$$

Assume now that $Ph_{x_k,q} \notin \mathcal{R}(PKP^*)$ for some $k = 1, \ldots, J$ and $q \in \mathbb{R}^2$. Then it follows that we can find

$$h \,\in\, \text{span}\{h_{x_j,p} \,:\, j = 1, \ldots, J\,,\; p \in \mathbb{R}^2\} \,\setminus\, \{0\}$$

with $Ph \perp \mathcal{R}(PKP^*)$. This means that Ph belongs to the null space of PKP^*, and since P is assumed to be injective on $\mathcal{R}(K)$ this implies that $KP^*(Ph) = 0$. Therefore we have

$$0 \,=\, \langle f, KP^*Ph\rangle \,=\, (PKf)\cdot(Ph)$$

for any $f \in L^2_\diamond(\partial D)$. Since $h \in \mathcal{R}(K)$ we can choose f to be the corresponding preimage to conclude that the Euclidean norm of Ph is zero, i.e., that $Ph = 0$. But since P is injective on $\mathcal{R}(K)$ this means that $h = 0$, which provides the desired contradiction and establishes (i).

To prove (ii) we note that (2.10) implies that if $Ph_{z,p} \in \mathcal{R}(PKP^*)$ then there exists h in (2.6) with $Ph_{z,p} = Ph$, and hence, the injectivity of P gives

$$h_{z,p} \,=\, h \,=\, \sum_{j=1}^{J} h_{x_j,p_j}$$

† In practice, of course, inclusions are small but not infinitesimal, and the algorithm tests whether $Ph_{z,p} \in \mathcal{R}(P(\Lambda_\varepsilon - \Lambda_0)P^*)$; see [8].

for certain dipole moments p_j, $j = 1, \ldots, J$. But then we necessarily have

$$u_{z,p} \,=\, \sum_{j=1}^{J} u_{x_j,p_j}$$

because the two functions on the left and right both satisfy the same Cauchy problem on ∂D for the Laplacian, and hence, comparing their singularities, we necessarily have $z \in \{x_j\}$ as claimed. □

We remark that this proposition (and its proof) is not restricted to the two-dimensional case considered in this work, but is valid for any finite space dimension. Further, without these injectivity assumptions both statements of the proposition no longer need to hold true; this will be exemplified in Section 4 below.

3. The main result

Theorem. *Let $D \subset \mathbb{R}^2$ be a bounded and simply connected Lipschitz domain, let K be defined as above, and P be given by* (2.7)*. Furthermore, assume that the number N of electrodes and J of inclusions satisfy the constraint $N > 2J + 2$. Then, if $z \in D$ and $p \in \mathbb{R}^2 \setminus \{0\}$, there holds*

$$Ph_{z,p} \in \mathcal{R}(PKP^*)\,, \qquad \textit{if and only if} \qquad z \in \{x_j\}\,. \tag{3.1}$$

Proof. By virtue of the proposition it is sufficient to show that P is injective on the subspace spanned by any given set of $J + 1$ insulated dipole potentials. For this we identify $\mathbb{R}^2$ with the complex plane and use complex variable techniques, i.e., by abuse of notation we identify the two-dimensional real spatial variable $x = (\xi, \eta) \in \mathbb{R}^2$ with the complex number $x = \xi + \mathrm{i}\eta \in \mathbb{C}$, and likewise for the other variables x_j, p, and z.

Consider first the case when D is the two-dimensional unit disk. In this case the insulated dipole potential $u_{z,p}$ of (2.4) can be written explicitly as

$$u_{z,p}(x) \,=\, \frac{1}{\pi}\,\mathrm{Re}\Big(\frac{p}{x-z} \,+\, \frac{\bar{p}x}{1-x\bar{z}}\Big)\,, \qquad x \in D\,, \tag{3.2}$$

the expression in paranthesis being real by itself for $x \in \partial D$, hence

$$h_{z,p}(x) \,=\, \frac{1}{\pi}\Big(\frac{p}{x-z} \,+\, \frac{\bar{p}x}{1-x\bar{z}}\Big)\,, \qquad x \in \partial D\,.$$

Now assume that $Ph = 0$ for any function of the form

$$h(x) \,=\, \frac{1}{\pi}\sum_{j=1}^{J+1}\Big(\frac{p_j}{x-x_j} \,+\, \frac{\bar{p}_j x}{1-x\bar{x}_j}\Big)\,. \tag{3.3}$$

By virtue of (2.7), (2.8) this implies that there exists $c \in \mathbb{R}$ such that

$$H_n \,=\, \frac{1}{|E_n|}\int_{E_n} h\,\mathrm{d}s \,=\, c$$

for all $n = 1, \ldots, N$, and some $c \in \mathbb{R}$, and hence, the rational function h of (3.3) attains the same value c at N different points on the unit circle (at least once on each piece E_n of the boundary covered by any of the electrodes). Since the numerator and denominator degrees of h are at most $2J + 2 < N$, each, this implies that $h \equiv c$; moreover, as each individual dipole trace has vanishing mean on ∂D, so has h, and therefore we conclude that $h \equiv 0$, which was to be shown.

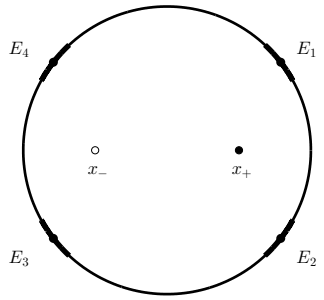

Figure 2. Sketch of the example of Section 4.

Assume next that D is an arbitrary simply connected Lipschitz domain in the complex plane and denote by ϕ a conformal map which takes D onto the unit disk. Moreover, denote by $\widehat{u}_{z,p}$ the insulated dipole potential (3.2) for the unit disk. Then, cf. [8], the insulated dipole potential $u_{z,p}$ in D with $z \in D$ and dipole moment p is given by

$$u_{z,p}(x) \,=\, \widehat{u}_{z',p'}(\phi(x)) \,+\, \gamma_z\,, \qquad x \in D\,,$$

where (in complex variables notation) $z' = \phi(z)$ and $p' = \phi'(z)p$; $\gamma_z \in \mathbb{R}$ is an additive constant (for fixed z) to satisfy

$$\int_{\partial D} u_{z,p}\,\mathrm{d}s \,=\, 0\,.$$

It follows that the trace of any linear combination h of $J+1$ insulated dipoles located in D is a rational function with numerator/denominator degree $2J+2$ at most of the variable $\phi(\,\cdot\,)$. Thus, as in the first part of the proof, if $Ph = 0$ then there are at least N points on the unit circle where this rational function has the same value $c \in \mathbb{R}$, from which we deduce that $h \equiv 0$. □

Note that for the if-part of this theorem $N = 2J+1$ electrodes are sufficient.

4. Examples

We complement our results with two illuminating examples, a theoretical and a numerical one.

First we show that the inequality $N > 2J+2$ occurring in the theorem is best possible in general. To this end we consider the unit disk D and the function

$$h(x) \,=\, h_{x_+,p_0}(x) - h_{x_-,p_0}(x) \,=\, \frac{2}{\pi}\Big(\frac{\mathrm{Re}\,(x-\xi)}{|x-\xi|^2} \,-\, \frac{\mathrm{Re}\,(x+\xi)}{|x+\xi|^2}\Big)$$

(using complex variables, again), which is the trace of the difference of two insulated dipoles located in $x_\pm = \pm\xi$ for some $\xi \in (0,1)$ with the same unit dipole moment p_0 oriented towards the positive real axis. It is easy to see that h is negative whenever $\mathrm{Real}\,(x) = \pm\xi$ and that

$$h(\pm 1) \,=\, \frac{2}{\pi}\Big(\frac{1}{1-\xi} \,-\, \frac{1}{1+\xi}\Big) \,>\, 0\,.$$

Accordingly, h must have four different zeros on the unit circle, the real parts of which are different from $\pm\xi$. We can therefore attach $N = 4$ electrodes to the unit circle in such a way that $Ph = 0$, i.e., that

$$Ph_{x_-,p_0} \,=\, Ph_{x_+,p_0}\,. \tag{4.1}$$

Note that $h_{x_\pm,p_0}$ are both symmetric with respect to the real axis and that h is also symmetric with respect to the imaginary axis. Hence, the roots of h are also symmetric with respect to both axes, and we can constrain the four electrodes to maintain this symmetry and to omit the points $\xi \pm \mathrm{i}\sqrt{1-\xi^2}$ and their reflections at the imaginary axis, compare Figure 2.

Assume next that we inject a current of one unit into the object through the two electrodes E_1 and E_2 in the positive real half plane, each, and extract the same amount of current at the other two electrodes, respectively; the corresponding boundary current is thus given by

$$f \,=\, P^* \begin{bmatrix} 1 \\ 1 \\ -1 \\ -1 \end{bmatrix},$$

and

$$u_0(x) \,=\, \frac{1}{\pi|E_1|} \int_{E_1} \log \frac{|x+e^{\mathrm{i}t}||x+e^{-\mathrm{i}t}|}{|x-e^{\mathrm{i}t}||x-e^{-\mathrm{i}t}|}\,\mathrm{d}t$$

is the associated reference potential for the homogeneous unit disk with conductivity $\sigma_0 \equiv 1$. Obviously, u_0 is symmetric with respect to the real axis and

$$\nabla u_0(x_\pm) \,=\, \alpha\, p_0 \qquad \text{for some } \alpha > 0\,. \tag{4.2}$$

Consider now the situation that x_+ is the location of the only inclusion within the unit disk, i.e., $J = 1$, and that this (small) inclusion has the shape $\mathcal{O}_+$ of a disk with positive conductivity $\sigma_+ \neq 1$ and area $|\mathcal{O}_+|$. Then [3, Theorem 2.1] yields

$$Kf \,=\, \lambda_+ h_{x_+,p_0}\,, \qquad \lambda_+ \,=\, 2\alpha\,|\mathcal{O}_+|\,\frac{1-\sigma_+}{1+\sigma_+}\,,$$

for the operator K of (2.3), and hence, by virtue of (4.1),

$$Ph_{x_-,p_0} \,=\, Ph_{x_+,p_0} \,=\, \frac{1}{\lambda_+}\,PKf \,=\, \frac{1}{\lambda_+}\,PKP^* \begin{bmatrix} 1 \\ 1 \\ -1 \\ -1 \end{bmatrix}.$$

In other words, the MUSIC algorithm would return x_- as a false-positive position of a second small inclusion, and hence, the second statement of the proposition and our theorem do not extend to this setting with $N = 2(J+1)$.

Consider next the situation that x_- is the position of a *second* disk shaped inclusion of the same size with conductivity $\sigma_- = 1/\sigma_+$, so that $N = 2J$. Then, cf. [3, Theorem 2.1] again, it follows from (4.2) that

$$Kf \,=\, \lambda_+ h_{x_+,p_0} \,+\, \lambda_- h_{x_-,p_0}$$

with λ_+ as before and

$$\lambda_- \,=\, 2\alpha\,|\mathcal{O}_+|\,\frac{1-\sigma_-}{1+\sigma_-} \,=\, -\lambda_+\,,$$

so that

$$PKP^* \begin{bmatrix} 1 \\ 1 \\ -1 \\ -1 \end{bmatrix} \,=\, PKf \,=\, \lambda_+ P\big(h_{x_+,p_0} \,-\, h_{x_-,p_0}\big) \,=\, 0$$

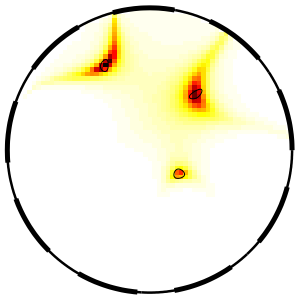

Figure 3. A numerical example with $N = 9$ electrodes and $J = 3$ inclusions.

by virtue of (4.1). Accordingly, $[1, 1, -1, -1]^T$ is a vector from the orthogonal complement of $\mathcal{R}(PKP^*)$. On the other hand, from the symmetry of h_{x_+,p_0} and (2.8) we conclude that

$$Ph_{x_+,p_0} = \begin{bmatrix} \beta \\ \beta \\ \gamma \\ \gamma \end{bmatrix} - \frac{\beta+\gamma}{2} \begin{bmatrix} 1 \\ 1 \\ 1 \\ 1 \end{bmatrix} = \frac{\beta-\gamma}{2} \begin{bmatrix} 1 \\ 1 \\ -1 \\ -1 \end{bmatrix}$$

for some $\beta > 0$ and $\gamma < 0$, which proves that $Ph_{x_+,p_0} \perp \mathcal{R}(PKP^*)$; the same result holds true for Ph_{x_-,p_0}. This shows that the first statement of the proposition is not valid in this example, for the MUSIC scheme fails to return either of the locations of the two inclusions, if the test is performed with the dipole moment p_0.

As a second example we have simulated data for $J = 3$ tiny inclusions in the unit disk, using $N = 9$ electrodes that cover 5/8 of the unit circle. Accordingly, the assumption $N > 2J + 2$ of our theorem is just fulfilled, and as we can see from Figure 3 the positions of the three inclusions are well reconstructed by the MUSIC scheme. The figure shows a color coded plot of the logarithm of the Euclidean norm of $(PKP^*)^{-1}Ph_{z,p}$ as a function of z; the 8×8 matrix PKP^* is nonsingular for this particular example, but is ill-conditioned with a condition number of the order of 10^5.

5. Discussion

It is obvious from the proof of our theorem that the same result applies to the point electrode model utilized in [10]; for the well-posedness of this model see [9], for example.

As far as the 3D case is concerned we note that in three space dimensions any linear combination in $\mathcal{R}(K)$ will have equipotential level curves on the surface ∂D; hence, for a given $h \in \mathcal{R}(K)$ it is easy to select any finite number of electrodes (whether these are point electrodes or given by bounded one or two-dimensional manifolds) for which $Ph = 0$. According to our proposition this means that no connection between the number N of electrodes and J of inclusions can hold in three space dimensions, so that Lechleiter's result may be the best possible achievement in that case.

Acknowledgement

The author is indebted to Dr. Stefanie Hollborn for valuable discussions of this material.

References

[1] Ammari H, Griesmaier R and Hanke M 2007 Identification of small inhomogeneities: Asymptotic factorization *Math. Comp.* **76** 1425–48

[2] Ammari H and Kang H 2007 *Polarization and moment tensors with applications to inverse problems and effective medium theory* (New York: Springer)

[3] Brühl M, Hanke M and Vogelius M S 2003 A direct impedance tomography algorithm for locating small inhomogeneities *Numer. Math.* **93** 635–54

[4] Cedio-Fengya D J, Moskow S and Vogelius M. S. 1998 Identification of conductivity imperfections of small diameter by boundary measurements. Continuous dependence and computational reconstruction *Inverse Problems* **14** 553–95

[5] Devaney A J 2000 *Super-resolution processing of multi-static data using time reversal and MUSIC* preprint

[6] Devaney A J 2012 *Mathematical Foundations of Imaging, Tomography and Wavefield Inversion* (Cambridge: Cambridge University Press)

[7] Hanke M 2013 *Factorizations all over the place* invited presentation at a workshop honoring Andreas Kirsch on the occasion of his 60th birthday

[8] Hanke M and Brühl M 2003 Recent progress in electrical impedance tomography *Inverse Problems* **19** S65–S90

[9] Hanke M, Harrach B and Hyvönen N 2011 Justification of point electrode models in electrical impedance tomography *Math. Models Meth. Appl. Sci.* **21** 1395–1413

[10] Lechleiter A 2015 The MUSIC algorithm for impedance tomography of small inclusions from discrete data *Inverse Problems* **31** 095004 (19pp)

[11] Mueller J L and Siltanen S 2012 *Linear and Nonlinear Inverse Problems with Practical Applications* (Philadelphia: SIAM)

[12] Therrien C W 1992 *Discrete Random Signals and Statistical Signal Processing* (Englewood Cliffs: Prentice-Hall)